

Extraction of density profile for near perfect multilayers

M. K. Sanyal, S. Hazra, J. K. Basu, and A. Datta

Surface Physics Division, Saha Institute of Nuclear Physics, 1/AF Bidhannagar, Calcutta 700064, India

(Received 29 January 1998; revised manuscript received 8 May 1998)

A simple inversion scheme, based on Born approximation, to determine the electron density profile of near perfect multilayers from specular x-ray reflectivity data has been presented. This scheme is useful for semiconductor multilayers and other thin films, which are grown almost according to the designed parameters. We also indicate the possibility of separating out the contribution of interdiffusion and roughness in electron density profiles of interfaces by utilizing information obtained from the analysis of diffuse scattering data. The extracted compositional profile was used to calculate structural details of epitaxial films along the growth direction. Simulated and metal organic vapor phase epitaxy grown InP/In_xGa_{1-x}As/InP quantum-well systems have been used to demonstrate this scheme. [S0163-1829(98)51232-5]

Specular reflectivity measurements of intense x-ray beams provide us with information regarding the electron density profile (EDP) of thin films as a function of depth, z .^{1,2} Measurements of the off-specular diffuse intensity, on the other hand, reveal in-plane morphology of the system and in turn provide us with information regarding roughness of various interfaces that may be present in the thin film, and correlation among these interfaces.² The specular reflectivity and diffuse scattering profiles are very sensitive to the EDP and the height-height correlation² of the interfaces, respectively. However, the extraction of EDP and height-height correlation from the measured specular and off-specular data through inversion techniques is nontrivial³ and is a subject of intense research.⁴ The problem with any such technique arises mainly due to loss of *phase information* during measurement, and several schemes⁴⁻¹⁰ have been suggested to overcome this *information loss*.

The advent of excellent growth techniques has enabled us to deposit multilayered thin films, especially those of epitaxial semiconductor systems, almost according to the designed parameters, viz. thicknesses with atomic monolayer precision and uniform composition over each layer.¹¹ Nevertheless, there still exist undesirable deviations in compositional and structural profiles of the deposited film from the designed parameters and a nondestructive characterization is highly desirable to improve the growth of these materials. A scheme has been presented here to extract the actual compositional and structural profile in the growth direction of these multilayer thin films from x-ray scattering measurements. In the present scheme the actual EDP is first calculated, with the desired profile as the initial guess, from diffuse-subtracted *true* specular reflectivity data. Information of correlated roughness¹² obtained from off-specular diffuse measurement is then used to extract the compositional depth profile. Diffraction data in (00 l) direction is then calculated using this compositional depth profile. In this communication the formalism is described first and then the merit of this ansatz is demonstrated using computer simulated and measured reflectivity profiles of quantum-well structures. Epitaxial In_xGa_{1-x}As (~ 100 Å) quantum well (with ~ 500 Å InP cap layer) structure grown on InP substrate by low-pressure metal organic vapor phase epitaxy (MOVPE) (Ref. 13) was

used here. X-ray scattering measurements were performed using a rotating anode Cu K $_{\alpha 1}$ source and a high precision goniometer.³

In Born approximation, reflectivity, $R(q)$, of a thin film is related to the xy averaged EDP, $\rho(z)$, through a Fourier transform as¹⁴

$$R(q) = R_F(q) \left| \frac{1}{\rho_\infty} \int_{-\infty}^{\infty} dz \rho'(z) \exp(iqz) \right|^2, \quad (1)$$

where ρ_∞ and $R_F(q)$ are the electron density and the Fresnel reflectivity of the substrate, respectively; $\rho'(z) = d\rho(z)/dz$ is the derivative profile; q is the wave vector in the film given by $q = \sqrt{q_z^2 - q_c^2}$, where $q_z = 2\pi/\lambda (\sin \alpha + \sin \beta)$. Here α and β are the incident and exit angles ($\alpha = \beta$ for specular reflectivity measurement) of the x-ray beam of wavelength λ , and q_c is the critical wave vector for the average film.

If we assume a model derivative profile, $\rho'_m(z)$, which is quite close to the actual derivative profile, $\rho'_e(z)$, that represents the experimentally observed reflectivity data, $R_e(q)$, then by taking simple ratio and by making a further assumption that these two derivative profiles are so close that the phase factor generated in the Fourier transform [given by Eq. (1)] for both observed reflectivity and model reflectivity profile, $R_m(q)$, are identical, one can write:

$$\rho'_e(z) = \mathcal{F}^{-1} \left[\sqrt{\frac{R_e(q)}{R_m(q)}} \mathcal{F}[\rho'_m(z)] \right]. \quad (2)$$

In the above expression \mathcal{F} and \mathcal{F}^{-1} are forward and inverse Fourier transform pair. In practice the above-mentioned phase factors are not equal and an iterative procedure using Eq. (2) is required to obtain the $\rho'_e(z)$ that represents $R_e(q)$, through intermediate derivative profiles generated in each iteration.

In analyzing the reflectivity data, an iterative procedure is started using Eq. (2), where we initially used model profile $\rho_m(z)$ to generate the profile $R_m(q)$. The deviation of $R_m(q)$ from $R_e(q)$ was used in Eq. (2) to generate modified profile, $\rho_e(z) [= \int_0^z dz \rho'_e(z)]$. Model reflectivity profile, $R_m(q)$, for the next iteration is now calculated by setting $\rho_m(z)$ equal to $\rho_e(z)$ of the previous iteration with the assumption that the

obtained derivative profile $\rho'_e(z)$ is nonzero only in the interval $(0, T)$, where T is the total thickness of the film. One can use either Parratt formalism¹ or Eq. (1) for calculating $R_m(q)$, and we found by simulation that in absence of absorption the same result can be obtained by both methods. Here we have used Parratt formalism because the absorption coefficients ($\sim 10^{-6} \text{ \AA}^{-1}$) are quite high for these quantum-well systems.

The iteration scheme suggested here can be considered as a box-refinement technique^{7,8} and convergence of such technique has been rationalized by Crowther.⁹ The obtained EDP within box $(0, T)$ from this iterative scheme can only be said to be consistent with the reflectivity and may not be a unique solution. However, recently some work¹⁰ is being done to resolve remaining ambiguities of the solution by using logarithmic dispersion relations and zeros of the reflectance. We shall not use these techniques here because the starting guess EDP is assumed to be very close to the solution and the iterative ansatz of Eq. (2) presumably converges to a solution whose phase is, in some sense, closest to the phase of the starting reflectance.

The diffuse scattering intensity as a function of wave vector $Q = (q_x, q_y, q_z)$ can be written in Born approximation as^{2,12}

$$I(q_x, q_z) = I_0 R(q) \frac{q_z}{2k_0 \sin \alpha} \int dx [\exp(q_z^2 C(x)) - 1] \times \exp(-iq_x x), \quad (3)$$

where I_0 is the direct beam intensity, $q_x = 2\pi/\lambda(\cos \beta - \cos \alpha)$, and $k_0 = 2\pi/\lambda$. In the above expression we assume¹² that all the interfaces are conformal and resolution out of the scattering plane is relaxed in such a way that integration over q_y has been performed during data collection. A Gaussian resolution function in q_x was used to convolute the $I(q_x, q_z)$ obtained from Eq. (3) before fitting the diffuse scattering data. The height-height correlation function for conformal self-affine rough interfaces^{2,12} was used here and can be written as

$$C_{ij}(x) \equiv C(x) = \langle z_i(0)z_j(x) \rangle = \sigma^2 \exp\left[-\left(\frac{x}{\xi}\right)^{2h}\right]. \quad (4)$$

Here, σ is the correlated rms roughness of the multilayer interfaces, ξ is the in-plane correlation length, and h is the roughness exponent.

In Born approximation the extended reflectivity around Bragg peaks, $R_B(q_z)$, can be written¹⁵ as

$$R_B(q_z) = \left[\sum_{n=0}^N A_n \exp\left[i\left(\sum_{j=0}^n d_j\right)q_z\right] + \frac{A_s \exp(iNd_s q_z)}{1 - \exp(id_s q_z)} \right]^2, \quad (5)$$

where the second term is for the substrate and the first term is for the epitaxial film having N layers with d_j and A_j as interplanar distance and scattering amplitude, respectively,¹⁵ for the j th atomic layer counting from the top of the film.

Before analyzing the experimental reflectivity data of the quantum well, we simulated similar reflectivity data from known EDP with Parratt formalism and analyzed these data using the present scheme and obtained the density profiles.

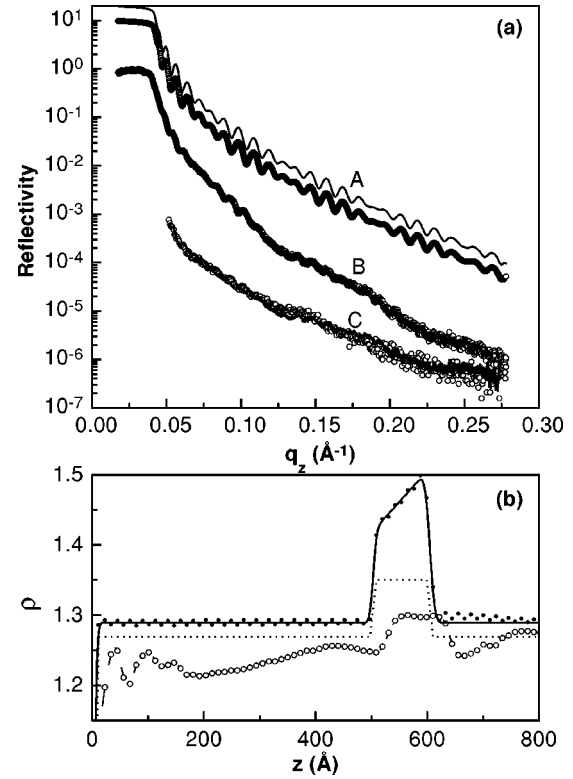


FIG. 1. (a) Specular reflectivity for model system ($\times 10$) (A), quantum-well sample (B), and longitudinal off-specular reflectivity for quantum-well sample (C). Parratt simulated and experimental data are shown by open circles and fitted curves by solid lines. Fitted curve for a model system has been shifted further ($\times 2$) as it exactly matches the simulated data. (b) Electron density profile (ρ , in electron/\AA^3) as a function of depth, z , for various systems are shown. The actual and obtained EDP for the model (shifted by $0.02 \text{ electron/\AA}^3$ for clarity) and fitted EDP for the experimental system are shown by solid lines, filled circles, and open circles, respectively. The initial EDP used for both simulated and experimental data is shown by a dotted line. The thickness of the cap layer and quantum well for the sample was found to be 528 and 112 \AA , respectively.

These profiles were then compared with the original EDP. These analyses reveal that the iterative procedure of the present scheme converges quite well even when the initial guess is quite far away from the solution. This is particularly interesting here because features in reflectivity data are not very prominent in these epitaxial systems with low electron density contrast at the interfaces. For all the simulation work $(q_z)_{\max}$ was taken as 0.28 \AA^{-1} which is the same as the experimental range here and hence $\rho_e(z)$ was obtained with 11.30 \AA slices. Although the reflectivity is required in each iteration for the evaluation of Eq. (2), we also calculated the complex reflectance to monitor the approach of the phase factor towards the correct value, known in simulation studies. One such analysis with simulated reflectivity profile [curve A, Fig. 1(a)] is shown along with the initial guess EDP and final EDP [Fig. 1(b)], having a slope of electron density in the quantum well. It is interesting to note that we could obtain the EDP using the above scheme almost exactly, including the rounding of the edges due to finite roughness, given by an error function. The presence of fluctuations of high spatial frequency are due to the finite cutoff in the

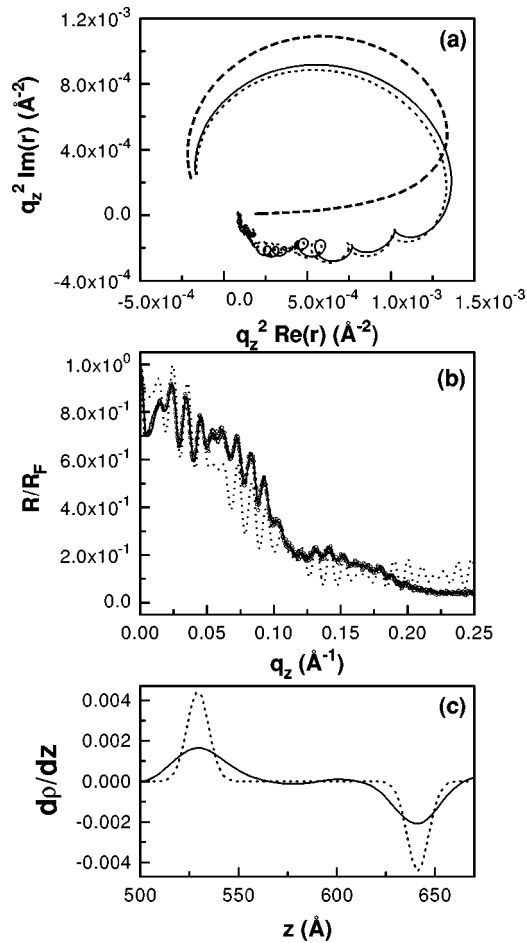


FIG. 2. (a) Phase variation as a function of q_z is shown by plotting the real and imaginary part of reflectance (r). The reflectance corresponding to Fresnel, initial, and final profile are shown by a dashed, dotted, and solid line, respectively. (b) Specular reflectivity normalized by Fresnel reflectivity as a function of q_z for experimental data (open circle), initial profile (dotted line), and final profile (solid line). (c) Derivative of final EDP (solid line) and Gaussian function with $\sigma = 5.5 \text{\AA}$ (dotted line) corresponding to the conformal rms interfacial roughness in the quantum-well region.

wave number range, as has also been observed in other inversion schemes.⁴ The best fit of the experimental reflectivity data (curve *B*) of the quantum-well system using the above scheme is shown in Fig. 1(a) along with the corresponding EDP [Fig. 1(b)]. The same profile was obtained with various initial guess profiles and it was confirmed that the presence of oscillatory electron density near the surface is essential to represent the hump in the reflectivity data near $q_z = 0.175 \text{\AA}^{-1}$. For clarity we have normalized all these reflectivity data with respect to the Fresnel reflectivity and have presented these data in Fig. 2(b). In this figure we have also shown [Fig. 2(a)] the real and imaginary parts of reflectance, for final and initial guess EDP, to indicate the nature of phase as a function of wave vector.¹⁶ It is instructive to note that the correct phase evolves iteratively; the phase for the Fresnel reflectivity of the substrate is also shown for comparison.

Analysis of the transverse diffuse data at three different q_z values using Eq. (3) (refer to Fig. 3) yields values of σ , ξ , and h as 5.5\AA , 10000\AA , and 0.45 , respectively. The same

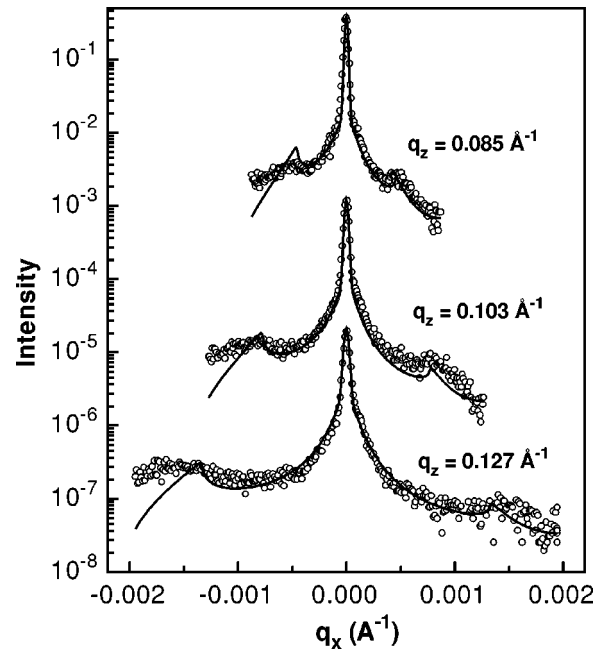


FIG. 3. Transverse diffuse scattering intensity (open circles) as a function of q_x for three different values of q_z for a quantum-well sample along with fit (solid line).

set of parameters was used to self-consistently calculate the longitudinal diffuse scattering profile [Fig. 1(a), curve *C*]. This profile follows the specular reflectivity profile (curve *B*) closely, indicating conformality.² It is known that EDP obtained from the x-ray specular reflectivity study is actually a convolution of compositional and interfacial roughness profiles. As the roughness here is conformal, one can obtain compositional profile by deconvoluting the $\rho'(z)$ with the Gaussian having $\sigma = 5.5 \text{\AA}$, corresponding to the interfacial roughness. This deconvolution can be performed in Fourier space by utilizing the fact that the Fourier transform of the convolution of two functions is the product of the Fourier transforms of the functions. A Gaussian-like (with variance

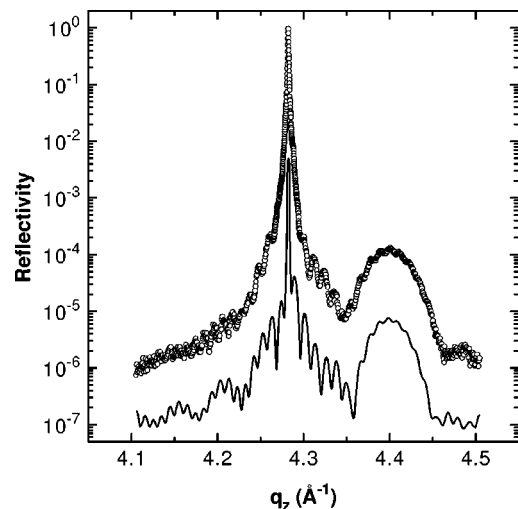


FIG. 4. Measured (open circles) and calculated ($\times 0.1$) (solid line) reflectivity around the (004) Bragg peak as a function of q_z for a quantum-well sample.

of σ_i) derivative profile of EDP is shown [Fig. 2(c)] along with the roughness Gaussian ($\sigma = 5.5 \text{ \AA}$), obtained from diffuse scattering analysis, at both the interfaces of the quantum well. The values of σ_i , found by fitting Gaussian functions, were 12 and 9 \AA for the quantum-well interfaces with the cap layer and substrate, respectively. This indicates that the interfacial profile is dominated by interdiffusion and substrate-quantum-well interface is sharper than the quantum-well cap-layer interface. It is also interesting to note that we obtained high in-plane correlation length for this epitaxial system having predominant interdiffusion, as observed earlier.¹⁷ Deconvoluted compositional profile is not presented here because the obtained profile is not much different from the EDP.

In Fig. 4 we have shown calculated and experimental (004) diffraction data. The lattice parameter of the quantum well obtained from the diffraction data is 5.71 \AA , which was used along with the obtained composition profile to extract the elemental composition. The composition near the center of the quantum well was found to be $\text{In}_{0.40}\text{Ga}_{0.60}\text{As}_{0.48}\text{P}_{0.52}$, which is quite different from the desired composition ($\text{In}_{0.33}\text{Ga}_{0.67}\text{As}$). A_j for the entire film was calculated from the obtained compositional profile and the values of d_j used

in the cap-layer (substrate) and quantum-well region were 1.467 and 1.427 \AA , respectively. All the main features observed in the experimental data could be obtained from this calculation. The detailed fitting of the diffraction data, including lattice strain profile at the interfaces for the quantum-well samples will be presented elsewhere.

In conclusion, we have presented an iterative inversion scheme, which is not a least-squares model fitting procedure, to extract EDP from reflectivity data. The compositional profile of a semiconductor multilayer was obtained by this scheme using additional information from diffuse scattering data analysis. The extracted compositional profile was used to calculate, in Born approximation, the extended reflectivity profile around the (004) Bragg peak of this epitaxial semiconductor multilayer. It should be mentioned here that the procedure presented here for specular data analysis can be used with suitable modification even for liquid and organic films where the specular and diffuse component of scattering cannot be clearly separated.¹⁸

We express our thanks to Professor B. M. Arora of the Tata Institute of Fundamental Research, Mumbai, India, for providing us with the sample.

- ¹L. G. Parratt, Phys. Rev. **95**, 359 (1954); M. Piecuch and L. Nevot, Mater. Sci. Forum **59-60**, 93 (1990); I. K. Robinson and D. J. Tweet, Rep. Prog. Phys. **55**, 599 (1992).
- ²S. K. Sinha, E. B. Sirota, S. Garoff, and H. B. Stanley, Phys. Rev. B **38**, 2297 (1988); M. K. Sanyal, S. K. Sinha, A. Gibaud, S. K. Satija, C. F. Majkrzak, and H. Homma, in *Surface X-Ray and Neutron Scattering*, edited by H. Zabel and I. K. Robinson, Springer Proceedings in Physics Vol. 61 (Springer-Verlag, Berlin, 1992), p. 91; V. Hóly and K. Baumbach, Phys. Rev. B **49**, 10 668 (1994).
- ³M. K. Sanyal, J. K. Basu, A. Datta, and S. Banerjee, Europhys. Lett. **36**, 265 (1996).
- ⁴J. Penfold and R. K. Thomas, J. Phys.: Condens. Matter **2**, 1369 (1990); in *Proceedings of the Workshop on Methods of Analysis and Interpretation of Neutron Reflectivity Data, Argonne, Ill, 1990*, edited by G. P. Felcher and T. P. Russel [Physica B, **173**, Nos. 1+2 (1991)]; X.-L. Zhou and S.-H. Chen, Phys. Rep. **257**, 223 (1995); R. Lipperheide, G. Reiss, H. Leeb, and S. A. Sofianos, Physica B **221**, 514 (1996).
- ⁵M. K. Sanyal, S. K. Sinha, A. Gibaud, K. G. Huang, B. L. Carvalho, M. Rafailovich, J. Sokolov, X. Zhao, and W. Zhao, Europhys. Lett. **21**, 691 (1993).
- ⁶C. F. Majkrzak and B. F. Berk, Physica B **221**, 520 (1996).
- ⁷L. Makovski, J. Appl. Crystallogr. **14**, 160 (1981).
- ⁸V. Skita, M. Filipkowskii, A. F. Garito, and J. K. Blasie, Phys. Rev. B **34**, 8526 (1986).
- ⁹R. A. Crowther, Acta Crystallogr., Sect. B: Struct. Crystallogr. Cryst. Chem. **B25**, 2571 (1969).
- ¹⁰G. Reiss and R. Lipperheide, Phys. Rev. B **53**, 8157 (1996); W. L. Clinton, *ibid.* **48**, 1 (1993); M. Li, M. O. Moller, H. R. Reb, W. Faschinger, and G. Landwehr, J. Phys. D **30**, 3296 (1997).
- ¹¹K. Ploog, in *Crystals: Growth, Properties and Applications*, edited by H. C. Freyhardt (Springer-Verlag, Berlin, 1980), Vol. 3, p. 75; T. Fukui and H. Saito, Jpn. J. Appl. Phys., Part 2 **23**, L521 (1984); Appl. Phys. Lett. **50**, 824 (1987).
- ¹²S. K. Sinha, M. K. Sanyal, S. K. Satija, C. F. Majkrzak, D. A. Neumann, H. Homma, S. Szpala, A. Gibaud, and H. Morkoc, Physica B **198**, 72 (1994).
- ¹³P. J. A. Thijs, E. A. Montie, and T. van Dongen, J. Cryst. Growth **107**, 731 (1991); R. T. H. Rongen, A. J. C. van Rijswijk, M. R. Leys, C. M. van Es, H. Vonk, and J. H. Wolter, Semicond. Sci. Technol. **12**, 974 (1997); M. K. Sanyal, A. Datta, S. Banerjee, A. K. Srivastava, B. M. Arora, S. Kanakaraju, and S. Mohan, J. Synchrotron Radiat. **4**, 185 (1997).
- ¹⁴J. Als-Nielsen, D. Jacquemann, K. Kjaer, F. Leveiller, M. Lahav, and L. Leseirowitz, Phys. Rep. **246**, 251 (1994).
- ¹⁵Y. Finkelstein, E. Zolotoyabko, M. Blumina, and D. Fekete, J. Appl. Phys. **79**, 1869 (1996).
- ¹⁶V. O. de Haan, A. A. van Well, P. E. Sacks, S. Adenwalla, and G. P. Felcher, Physica B **221**, 524 (1996).
- ¹⁷P. M. Reimer, J. H. Li, Y. Yamaguchi, O. Sakata, H. Hashizume, N. Usami, and Y. Shiraki, J. Phys.: Condens. Matter **9**, 4521 (1997); J. Stetner, L. Schwalowsky, O. H. Seeck, M. Tolan, W. Press, C. Schwarz, and H. v. Kanel, Phys. Rev. B **53**, 1398 (1996).
- ¹⁸M. K. Sanyal, S. K. Sinha, K. G. Huang, and B. M. Ocko, Phys. Rev. Lett. **66**, 628 (1991); J. K. Basu and M. K. Sanyal, *ibid.* **79**, 4617 (1997).